Influence of Inert Gas Boundaries on Detonation Propagation

Youssef K. Wahba
McGill University
Montreal, Quebec, Canada

Xiaocheng Mi
Eindhoven University of Technology
Eindhoven, the Netherlands

Charles B. Kiyanda
Concordia University
Montreal, Quebec, Canada

Andrew J. Higgins
McGill University
Montreal, Quebec, Canada

1 Introduction

Detonation propagation dynamics vary depending on the confining medium. Recently, there has been growing interest in understanding the dynamics of detonation propagation when bounded by inert gases. While this problem has been experimentally and analytically investigated in the earlier works of [1–3], recent work [4–6] has revisited this problem owing to its relevance to flows encountered in rotating detonation engines (RDEs). In RDEs, detonations propagate in an annular chamber and are surrounded by the high temperature combustion products that are left from the previous cycles. Early work by Sommers and Morrison [2] highlighted the occurrence of an oblique shock trailing behind the detonation when interacting with an inert layer. The study assumed that the CJ plane coincided with the shock plane, resulting in the detonation propagating at the CJ speed. Subsequent work by Dabora et al. [1] considered the effects of area divergence in the reaction zone and identified a velocity deficit in such detonations. Further experimental work by Adams [3] highlighted the existence of a *precursor shock* when an explosive mixture was bounded by a lighter, inert gas, such as helium. The type of wave interaction that occurs is therefore dependent on the acoustic impedance ratio between the inert gas and the reactive mixture. Simulations performed by Houim and Fievisohn [4] showed that this precursor shock can be obtained when the acoustic impedance ratio between the inert and the reactive media is low enough. An analytical model was presented by the present authors in [7] to study this precursor shock phenomenon with varying acoustic impedance ratios. The model demonstrated strong agreement with CFD simulations, primarily due to the use of non-Arrhenius chemical kinetics, resulting in cell-free detonation fronts and a stable reaction zone. However, the study employed a reflective boundary above the inert layer, which choked the flow and limited the model's applicability to RDE flows. This study extends the work of [7] in two ways: first accounting for the cellular nature of detonations using Arrhenius kinetics, and second by better mimicking conditions more relevant to RDEs through the use of a transmissive boundary condition above the inert layer.

Correspondence to: youssef.wahba@mail.mcgill.ca

2 Numerical methodology and simulation setup

The two-dimensional, inviscid, reactive Euler equations are solved using the second-order accurate MUSCL-Hancock scheme with a van Leer limiter. A CFL of 0.8 is maintained throughout the study. The thermodynamic variables are nondimensionalized with respect to the state of the unburned mixture ahead of the detonation. A simple, single-step reaction, and a one-gamma model (γ = constant) is used throughout the study. The reaction progress variable, λ, varies from 0 in the unburnt state to 1 for fully burnt. Section 3.1 presents the results obtained using non-Arrhenius kinetics, whereas Section 3.2 provides simulation results based on Arrhenius kinetics, incorporating the multidimensional effects of the detonation. Section 3.3 presents the results using a transmissive boundary condition above the inert layer. The nondimensional input parameters used were γ = 1.3, Q = 23.0, the pressure and temperature of the initiation region were set to $2P_{\mathrm{CJ}}$ and $2T_{\mathrm{CJ}}$, respectively. For the Arrhenius simulations, $\frac{E_{\mathrm{a}}}{RT_0}$ was set to 15, and the chemical kinetics parameters were chosen such that approximately six detonation cells were observed in the reactive layer, with k = 1.75.

$$\mathbf{U} = \begin{pmatrix} \rho \\ \rho u \\ \rho v \\ \rho e \\ \rho\lambda \end{pmatrix}, \quad \mathbf{F} = \begin{pmatrix} \rho u \\ \rho u^2 + p \\ \rho uv \\ (\rho e + p)u \\ \rho\lambda u \end{pmatrix}, \quad \mathbf{G} = \begin{pmatrix} \rho v \\ \rho uv \\ \rho v^2 + p \\ (\rho e + p)v \\ \rho\lambda v \end{pmatrix}, \quad \mathbf{S} = \begin{pmatrix} 0 \\ 0 \\ 0 \\ 0 \\ \rho\dot{\lambda} \end{pmatrix} \tag{1}$$

$$e = \frac{p}{(\gamma - 1)\rho} + \frac{(u^2 + v^2)}{2} + \lambda Q \tag{2}$$

$$\dot{\lambda} = k(1 - \lambda) \quad \text{or} \quad \dot{\lambda} = k(1 - \lambda)e^{-\frac{E_{\mathrm{a}}}{RT}} \tag{3}$$

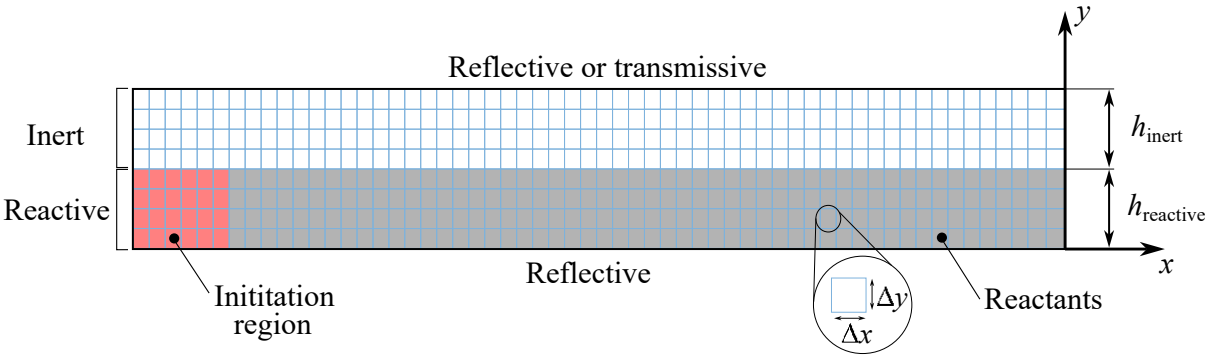

Figure 1: Numerical grid for initiation

The pressures in the inert and reactive layers were initially set equal, meaning the acoustic impedance ratio, Z, between the inert and reactive layer depended solely on their respective temperatures, expressed as:

$$Z = \sqrt{\frac{T_{\mathrm{Reactive}}}{T_{\mathrm{Inert}}}} \tag{4}$$

Section 3 presents three simulations with $Z = 0.45$ and one with $Z = 0.27$, exploring different reaction rate models and top boundary conditions. A summary of the initial conditions is provided in Table 1.

Table 1: Summary of simulation cases in this study

Case #	Reaction Model	Top BC
Case 1	$\dot{\lambda} = k(1-\lambda)$	Reflective
Case 2	$\dot{\lambda} = k(1-\lambda)e^{-\frac{E_a}{RT_0}}$	Reflective
Case 3	$\dot{\lambda} = k(1-\lambda)$	Transmissive

3 Results and discussion

3.1 Case 1: Instant burn rate

In order to facilitate comparison to an exact, analytic solution of the flowfield, the case of an instant burn rate was considered. In this case, the detonation front is stable and the absence of cellular structure makes the flowfield more amenable to modelling. The analytical solution for a detonation propagating in a medium surrounded by inert gas and bounded by a reflective wall was derived using the velocity of a two-layer detonation, as presented in [8]. A polar analysis was performed where the discontinuities intersect in the reactive layer in order to evaluate the wave and deflection angles involved in the flow. The height of the detonative Mach stem was determined using geometric relations outlined in [9], which are analogous to those observed in overexpanded nozzles. Figure 2 illustrates the regions where the flow has reacted in the simulations, indicating the presence of a nonreactive oblique shock transmitted into the reactive layer. Figure 3 presents the analytical solution overlaid on the numerical Schlieren derived from the CFD simulation.

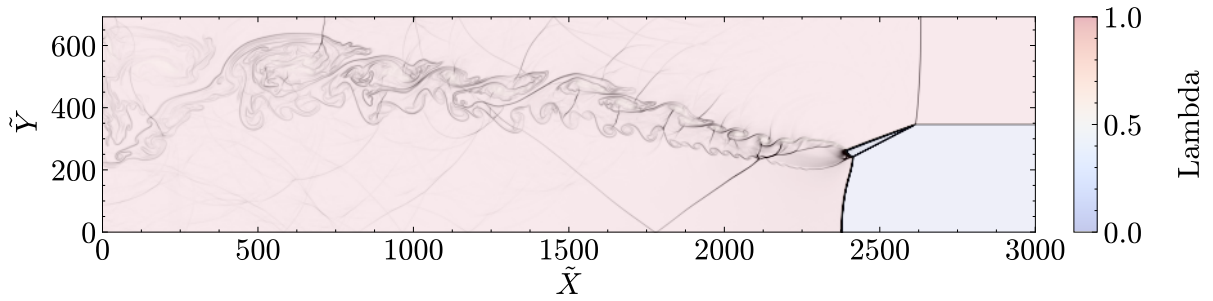

Figure 2: λ overlay, Z = 0.45 (reproduced from [7])

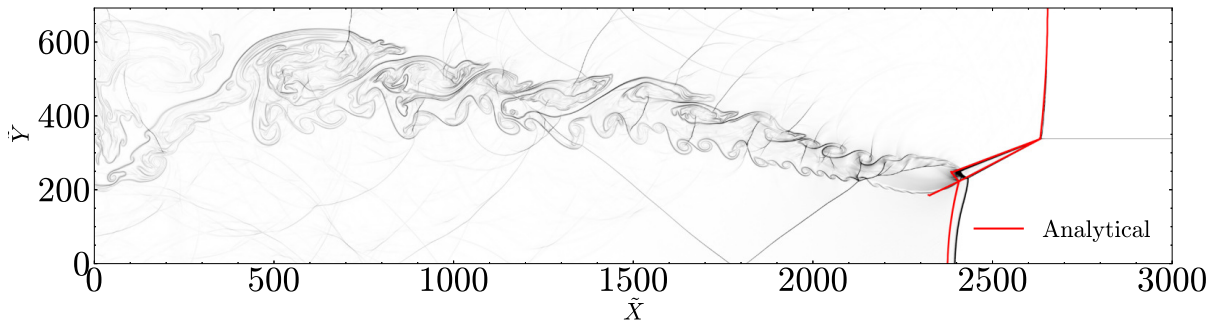

Figure 3: Analytical solution superimposed on CFD, Z = 0.45 (reproduced from [7])

3.2 Case 2: Arrhenius kinetics

For the Arrhenius simulations, approximately six detonation cells were developed across the reactive layer, as shown in Fig. 4, which shows the maximum pressure histories of the detonation. The qualitative features remained similar to the previous case, where the precursor shock continues to propagate ahead of the detonation, and a nonreactive oblique shock is transmitted into the reactive layer, as shown in Fig. 5. However, unlike the previous case, a shock-induced combustion occurs instead of the weak overdriven oblique detonation previously analyzed, leading to greater deviation between the analytical solution and the CFD results. The propagation of the detonation, while confined by the inert layer, is governed by $\frac{E_a}{RT_0}$, as well as the height of the reactive layer, h_{reactive}.

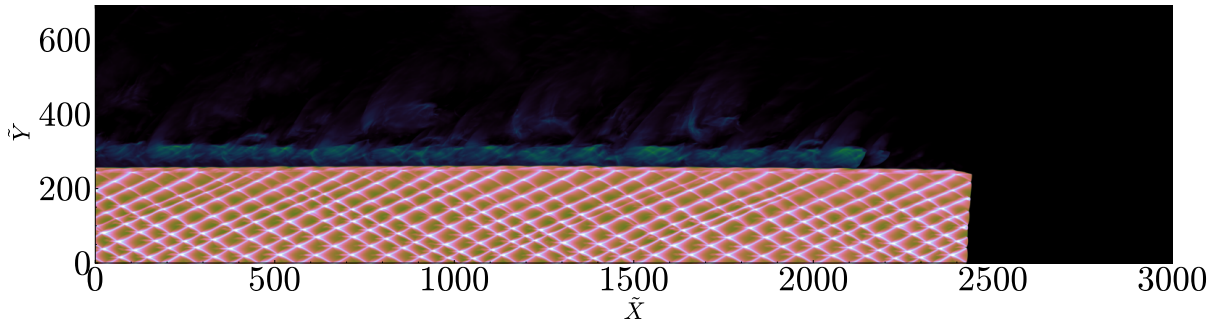

Figure 4: Numerical soot foil, $Z = 0.45$

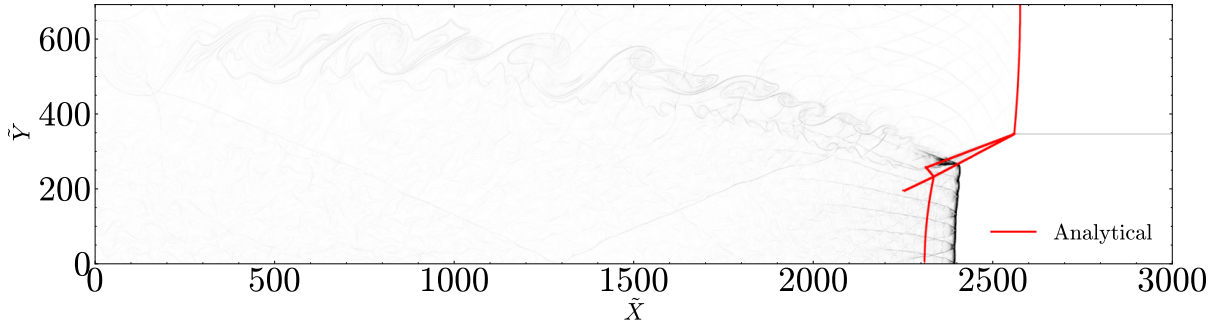

Figure 5: $Z = 0.45$ with Arrhenius kinetics

3.3 Case 3: Transmissive boundary

The prior cases considered an inert layer bounded by a rigid wall. In Case 3, the upper boundary is made transmissive, resulting in a flowfield more similar to that of a rotating detonation engine where the combustion products are free to expand through an exhaust from the combustion chamber. At high impedance ratios, the detonation experiences minor losses due to the area divergence within the reaction zone. The velocity deficit of the detonation can vary depending on the chemical kinetics and the length of the reaction zone. In the case of an infinitely thin reaction zone, the detonation speed approaches the CJ speed of the mixture, and the CJ plane can be assumed to align with the shock plane, as noted in [2]. A schematic of the typical wave structure is presented in Fig. 6a. In this figure, the combustion products expand through a Prandtl-Meyer fan after exiting the CJ plane, matching the pressure and flow direction behind an oblique shock transmitted into the inert layer. The wave structure of this *attached oblique shock* configuration is steady, and the solution for the oblique shock angle and flow deflection is

determined by locating the intersection point between the expansion polar and the oblique shock polar, as noted in [10]. As the acoustic impedance ratio decreases, the Mach number in the inert layer also decreases, causing the oblique shock polar to *shrink* until it detaches from the expansion polar, resulting in the formation of a precursor shock, as seen in [4]. For the case of $Z = 0.45$, the oblique shock polar, represented by the blue line in Fig. 6b, still intersects the expansion polar. Consequently, a solution is obtained where the oblique shock propagates behind the detonation into the inert layer, as demonstrated in the CFD simulation shown in Fig. 7. Reducing the acoustic impedance ratio to a value below 0.30 will lead to a precursor shock moving ahead of the detonation, as shown in Fig. 8.

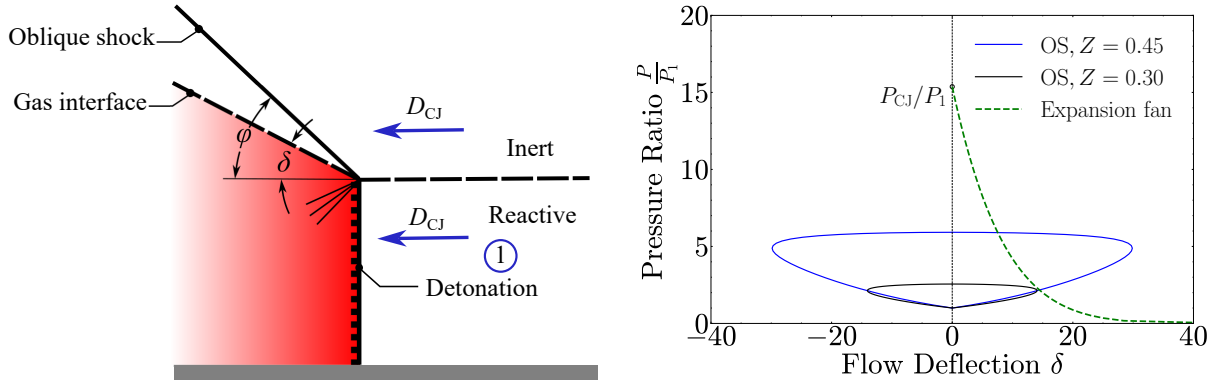

(a) Attached oblique shock schematic with CJ plane coinciding with shock front

(b) Polar analysis showing the onset of a detached shock at $Z < 0.30$

Figure 6

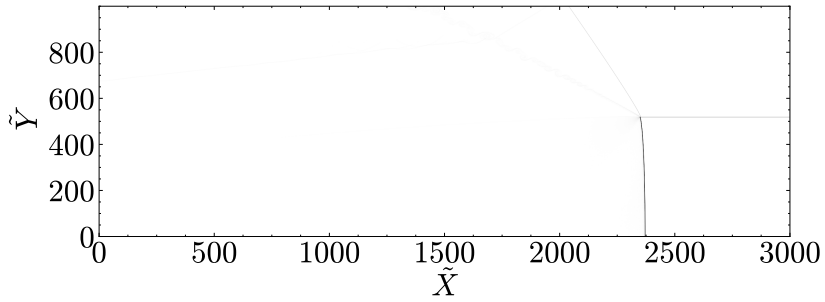

Figure 7: Pseudo-Schlieren of a detonation confined by an inert layer ($Z = 0.45$) with a transmissive boundary

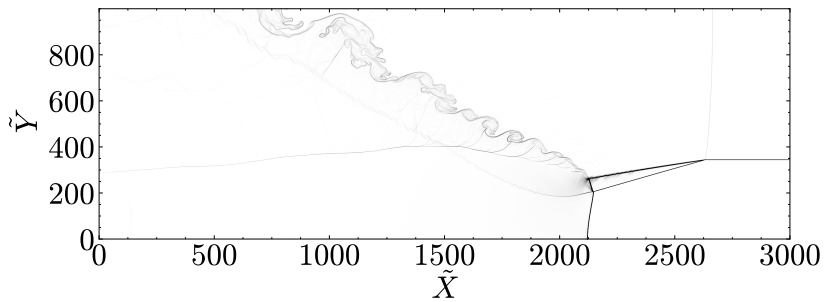

Figure 8: Pseudo-Schlieren of a detonation confined by an inert layer ($Z = 0.27$) with a transmissive boundary

4 Conclusion and future work

As more complex cases are examined—from a stable burn-rate model to an unstable Arrhenius rate model and eventually incorporating a transmissive boundary—the structure of the leading shock- and detonation-front complex continued to lend itself to analytic polar analysis. For a boundary of inert gas with a lower acoustic impedance than the detonable layer, this analysis predicts the existence and structure of a precursor wave that is able to alter the state of the detonable layer prior to the arrival of the detonation wave. The inert boundary of low-impedance gas is a good surrogate for the layer of combustion products bounding the detonable layer in a rotating detonation engine. This finding implies that an analytic, polar-based model possesses potential for aiding in the prediction and analysis of flowfields present in rotating detonation engines.

References

[1] Dabora EK, Nicholls JA, Morrison RB. (1965). The influence of a compressible boundary on the propagation of gaseous detonations. Proc. Combust. Inst. 10: 1965.

[2] Sommers, WP, Morrison, RB. (1962). Simulation of Condensed-Explosive Detonation Phenomena with Gases. Phys. Fluids. 5: 241.

[3] Adams, TG. (1972). Experimental investigation of the interaction of a detonation wave with a boundary gas. PhD Thesis. Michigan State University.

[4] Houim, RW, Fievisohn, RT. (2017). The influence of acoustic impedance on gaseous layered detonations bounded by an inert gas. Combust. Flame. 179: 185–198.

[5] Menezes, M, Ciccarelli, G, Chapdelaine, S. (2024). Numerical study of detonation propagation in a semi-confined nonuniform layer bound by an inert gas. Int. J. Hydrogen Energy. 49: 1223–1231.

[6] Cheevers, K, Yang, H, Raut, M, Hong, Z, Radulescu, M. (2023). A flame technique to isolate the detonation/product interface relevant to rotating detonation engines. Proc. Combust. Inst. 39(3): 3095–3105.

[7] Wahba, YK, Mi, XC, Kiyanda, C, Higgins, AJ. (2025). Analysis and simulation of a detonation bounded by a low impedance gas. AIAA SCITECH 2025 Forum, AIAA Paper 2025-1965.

[8] Mitrofanov, VV. (1976). Detonation in two-layer systems. Acta Astronautica. 3(11): 995–1004.

[9] Paramanantham, V, Janakiram, S, Gopalapillai, R. (2022). Prediction of Mach stem height in compressible open jets. Part 1. Overexpanded jets. J. Fluid Mech. 942: A48.

[10] Shepherd, JE, Kasahara, J. (2017). Analytical models for the thrust of a rotating detonation engine. GALCIT Report FM2017.001.